Recent progress in ligand photorelease reaction mechanisms: Theoretical insights focusing on Ru(II) 3MC states

Adrien Soupart, Fabienne Alary, Jean-Louis Heully, Paul I Elliott, Isabelle M. Dixon

Coord. Chem. Rev. 2020, 408, 213184.
https://doi.org/10.1016/j.ccr.2020.213184

Recent progress in ligand photorelease reaction mechanisms: theoretical insights focusing on Ru(II) ^{3}MC states[§,♯]

Adrien Soupart[a], Fabienne Alary[a], Jean-Louis Heully[a], Paul I.P. Elliott[b,c], Isabelle M. Dixon[a]*

[a] Laboratoire de Chimie et Physique Quantiques, UMR 5626 CNRS/Université Toulouse 3 - Paul Sabatier, Université de Toulouse, 118 route de Narbonne, Toulouse, 31062, France

[b] Department of Chemistry, University of Huddersfield, Huddersfield, HD1 3DH, UK

[c] Centre for Functional Materials, University of Huddersfield, Huddersfield, HD1 3DH, UK

*Corresponding author: isabelle.dixon@irsamc.ups-tlse.fr

[§] This work was presented at the 23rd edition of the *International Symposium on the Photophysics and Photochemistry of Coordination Compounds* in Hong Kong

[♯] *Dedicated to Jean-Pierre Sauvage on the occasion of his 75th birthday*

Abstract

The elucidation of reaction mechanisms taking place in the excited state is a current challenge for experimental and theoretical chemists. Ru(II) complexes have a long history for photophysics, and there is currently an increasing interest in their photochemistry. Ru(II) complexes provide a vast field of exploration, whether for synthetic purposes, to trigger molecular motions or to release biologically active components. The excited states involved, especially those of MLCT and MC character, are key to the rationalization of their photophysical and photochemical properties. This review focuses on the recent progress in the latter field through several case studies: i) the archetypes $[Ru(bpy)_3]^{2+}$ and$[Ru(tpy)_2]^{2+}$ first serve for the validation of the theoretical methods we are using; ii) then the study of photorelease of a monodentate ligand provides us with novel mechanistic hypotheses; iii) one step further, studying the photorelease mechanism of a bidentate ligand provides us with novel ^{3}MC states of peculiar flattened geometry; iv) finally, returning to $[Ru(bpy)_3]^{2+}$ itself, we will show that the existence of these states can be generalized and probably represent a major player in the description of photoreactivity mechanisms, for ruthenium and possibly several other transition metals.

Coord. Chem. Rev. 2020, 408, 213184.
https://doi.org/10.1016/j.ccr.2020.213184

Keywords

photoreactivity mechanisms; inorganic photochemistry; theoretical chemistry; DFT; potential energy surfaces; metal-centered excited states

Coord. Chem. Rev. 2020, 408, 213184.
https://doi.org/10.1016/j.ccr.2020.213184

1. Introduction

The interplay between the metal-to-ligand charge transfer (MLCT) and metal-centred (MC) excited states of Ru(II) complexes is at the heart of modern inorganic photochemistry. These two states are the key protagonists towards both the photophysical (photoluminescence, photoinduced electron or energy transfer) and photochemical (photoisomerization, photorelease) properties of this family of compounds, the balance of which is crucial in terms of potential applications. Photostability is indeed a critical issue for photophysical applications (e.g. photosensitizing for photodynamic therapy [1][2][3][4], photocatalysis [5][6][7], sensing and imaging [8], or solar energy conversion [9]), while the opposite is sought for photochemical applications [10] such as synthetic purposes [11][12][13][14], photorelease of biologically active moieties [15][16][17][18][19] or phototriggered molecular machines [20].

Several experimental and theoretical studies have contributed to providing valuable information in terms of microscopic mechanistic details relevant to ligand photorelease from Ru(II) complexes [21][22][23][24][25][26][27][28][29][30][31][32][33][34][35][36]. However they also highlight the intrinsic complexity of studying multistep light-induced reactions under experimental conditions that affect the reaction course, particularly solvent [37]. Major gaps remain in this field, and this review aims at summarizing our recent contributions via joint experimental-theoretical studies. Our knowledge of the topology of the ground potential energy surface (^{1}PES) and of the lowest triplet potential energy surface (^{3}PES) has gradually improved to a point where we can now build up and propose multistep photorelease reaction mechanisms along with the microscopic description of the states involved.

2. Context and theoretical methods: ^{3}MC-mediated excited state deactivation in $[Ru(bpy)_3]^{2+}$ and $[Ru(tpy)_2]^{2+}$ as an illustration

Thermal ligand exchange is a key contributor to the function of metalloenzymes in Nature [38]. Photochemical ligand release, on the other hand, is specific to thermally stable compounds and can be triggered at will with efficient time, energy and space selectivities. The establishment of photoreactivity mechanisms implies that one has a good knowledge of all the different excited states that are (susceptible to be) populated following light irradiation.

In the case of Ru(II) complexes such as those described here, the available ground and excited states and the interconversions between them are commonly described using a Jablonksi diagram (Figure 1a). For these complexes, the presence of π-accepting ligands such as polypyridines ensures the presence of low-lying ^{1}MLCT states that will provide light-absorption capabilities in the visible region of the electromagnetic spectrum. Following fast and quantitative intersystem crossing [39][40], ^{3}MLCT states are populated within in a few hundreds of fs [41]. ^{3}MLCT states are thus the first ones to be scrutinized, the radiative deactivation of which can be modeled using a variety of theoretical methods. Some of them take into account the spin orbit coupling (SOC) between the lowest ^{3}MLCT state and the ground state, allowing electronic states of different spin multiplicity to couple. For $[Ru(bpy)_3]^{2+}$ (bpy = 2,2'-bipyridine) we have shown that the emissive MLCT state is predominantly triplet in character, to such an extent that excited state energies with or without SOC are similar within the accuracy of the method [42]. Another method takes into account the vibrational coupling between the emitting state and the ground state and is a powerful tool for modeling experimental emission band envelopes. Indeed, theoretical Vibrationally Resolved Electronic Spectroscopy (VRES) [43][44] is in excellent agreement with the experimental emission data for $[Ru(bpy)_3]^{2+}$ [45], and also allows a very subtle analysis of the vibronic fine structure (see ref [46] for an example in absorption spectroscopy), the interpretation of which being particularly challenging in the absence of a theoretical model.

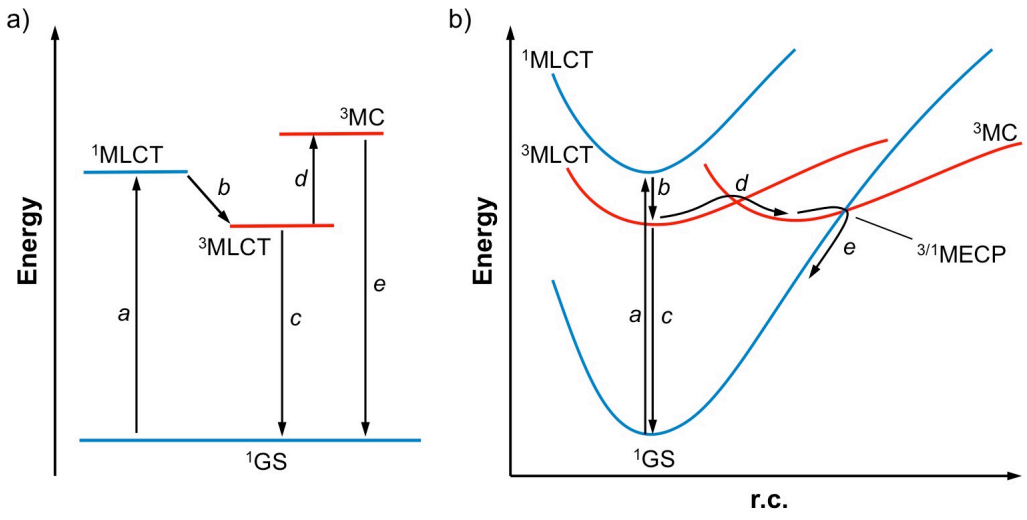

Figure 1. (a) Jablonski diagram depicting the ground and excited states of a $[Ru(bpy)_3]^{2+}$-like complex (key processes: a photoexcitation, b intersystem crossing, c radiative deactivation, d internal conversion, e non

radiative deactivation), and (b) the corresponding potential energy surface description (r.c. = reaction coordinate).

^{3}MLCT states can also deactivate nonradiatively, either by direct surface crossing with the ground state (e.g. for Ru(II) cyclometallated complexes [47]) or through heat transfer to their environment [37][48]. They may also undergo internal conversion to ^{3}MC states, the latter being held responsible both for efficient nonradiative deactivation and chemical decomposition. As ^{3}MC states are associated with the population of an antibonding dσ* orbital, significant Ru-N bond elongations occur [49]. The simple Jablonski diagram does not take into account such structural deformations and therefore only offers a partial representation of the system. A more global picture is brought by a potential energy surface description, in which the structural deformations that characterise ^{3}MC states can be regarded as the reaction coordinate (Figure 1b).

As the archetypical $[Ru(bpy)_3]^{2+}$ (Figure 2) is rather photostable, and $[Ru(tpy)_2]^{2+}$ (tpy = 2,2':6',2''-terpyridine) is truly [50], we will first focus on the nonradiative deactivation of their ^{3}MC states. To do so, the minimum energy crossing point ($^{3/1}$MECP, Figure 1b) between the singlet and the triplet PES should be optimized [51][52]. The similarities, both in structure and energy, to the corresponding ^{3}MC state and the topology of the crossing itself (from almost parallel to almost perpendicular surfaces) are important to the efficiency of nonradiative deactivation [53][54].

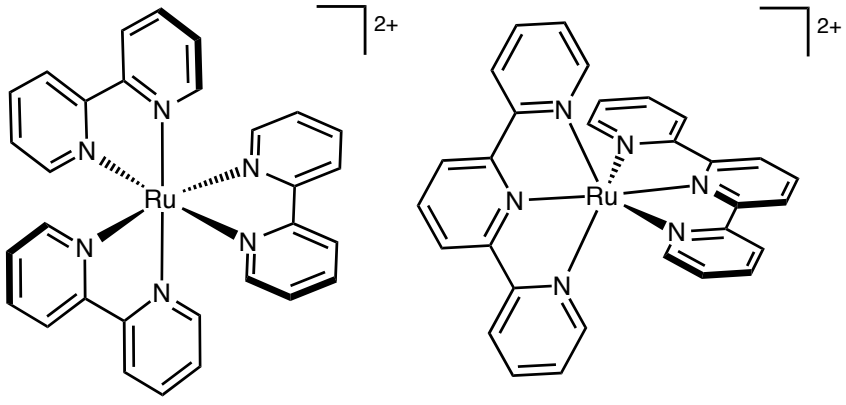

Figure 2. Structures of $[Ru(bpy)_3]^{2+}$ and $[Ru(tpy)_2]^{2+}$.

Regarding the internal MLCT-MC conversion process itself, consisting in an electron transfer from a ligand-based π* orbital to a metal-based dσ* orbital, this can be probed theoretically by optimizing the transition state that connects these two minima [55][56][57] or, in a more

approximate fashion, by running a relaxed surface scan along a user-defined reaction coordinate [23][58][59], in this case Ru-N bond elongation along one N-Ru-N axis. Alternatively, the minimum energy path (MEP) can be computed using a method such as the Nudged Elastic Band (NEB) [60][61], which is the one we have been using for several years. The NEB method starts from an initial path connecting two geometries. Relaxation of this initial path leads to the MEP through path gradient and tangent information. This method displays the great advantage over a relaxed surface scan that the reaction coordinate is user-independent, being initially mathematically defined (IDPP method in our case [62]) and, along the converged path, being the actual physical reaction coordinate. The highest energy point along the MEP also provides an excellent guess for transition state optimization. Until now the NEB method has scarcely been used in molecular chemistry but it has proved very powerful in our hands. Its implementation within more and more quantum chemistry codes certainly promises a bright future to it.

To illustrate and validate the use of these methods in the context of inorganic photochemistry, we have confronted the available experimental data with our computed data for the archetype complexes $[Ru(bpy)_3]^{2+}$ and $[Ru(tpy)_2]^{2+}$ (Figure 2). $[Ru(bpy)_3]^{2+}$ (as well as 2,2'-bipyrazine and 1,4,5,8-tetraazaphenanthrene complexes) were initially studied in vacuum under symmetry constraints for obvious matters of computational resources [49][63][42]. Nowadays these technical restrictions no longer apply on such molecular systems, which is why the states discussed in this review were optimized in implicit solvent without symmetry. In line with the occupation of a dσ* orbital in the ^{3}MC state, major bond elongations are observed in such structures: two elongations in the case of the tris(bidentate) complex, four elongations in the case of the bis(terdentate) one (Figure 3).

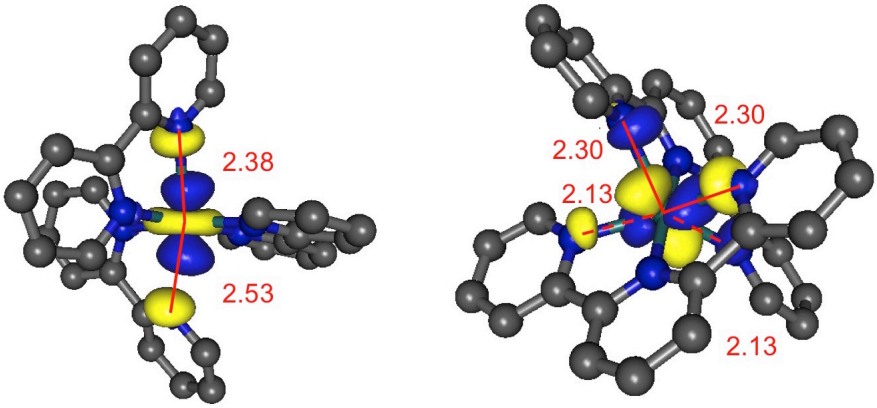

Coord. Chem. Rev. 2020, 408, 213184.
https://doi.org/10.1016/j.ccr.2020.213184

Figure 3. ^{3}MC state of $[Ru(bpy)_3]^{2+}$ and $[Ru(tpy)_2]^{2+}$ with their SOMO+1 and the corresponding key Ru-N elongations (distances in Å).

The optimization of the ^{3}MLCT and ^{3}MC minima provides us with Jablonski diagrams for the two complexes that display similar ^{3}MLCT energies (46-47 kcal/mol with respect to the ground state) and similar ^{3}MLCT-^{3}MC energy gaps (3-4 kcal/mol) [45]. Rationalization of the room temperature luminescence of $[Ru(bpy)_3]^{2+}$ versus the nonluminescence of $[Ru(tpy)_2]^{2+}$ thus requires us to go beyond this Jablonski diagram. Computation of the minimum energy path for the ^{3}MLCT-^{3}MC conversion gives an activation energy of 9 kcal/mol for bpy but only 4 kcal/mol for tpy, in line with a more efficient population of the ^{3}MC state in the tpy case. In addition, these activation energies compare remarkably well with those obtained from variable temperature luminescence lifetimes measurements (11 kcal/mol for $[Ru(bpy)_3]^{2+}$ [64] and 5 kcal/mol for $[Ru(tpy)_2]^{2+}$ [65]). Finally, optimization of the $^{3/1}$MECPs shows that the ^{3}MC-$^{3/1}$MECP energy gap is 6 kcal/mol for bpy but only 1 kcal/mol for tpy, in line with the much smaller geometrical distortions observed between the ^{3}MC state and the $^{3/1}$MECP for tpy. Nonradiative deactivation is thus expected to be much more favourable and efficient for $[Ru(tpy)_2]^{2+}$ than for $[Ru(bpy)_3]^{2+}$. Combining minima and MECP optimization with the computation of the minimum energy path for internal conversion on the ^{3}PES (Scheme 1) has overall provided us with the rationalization of the photophysical properties of the two major archetypes of Ru(II) photochemistry [45].

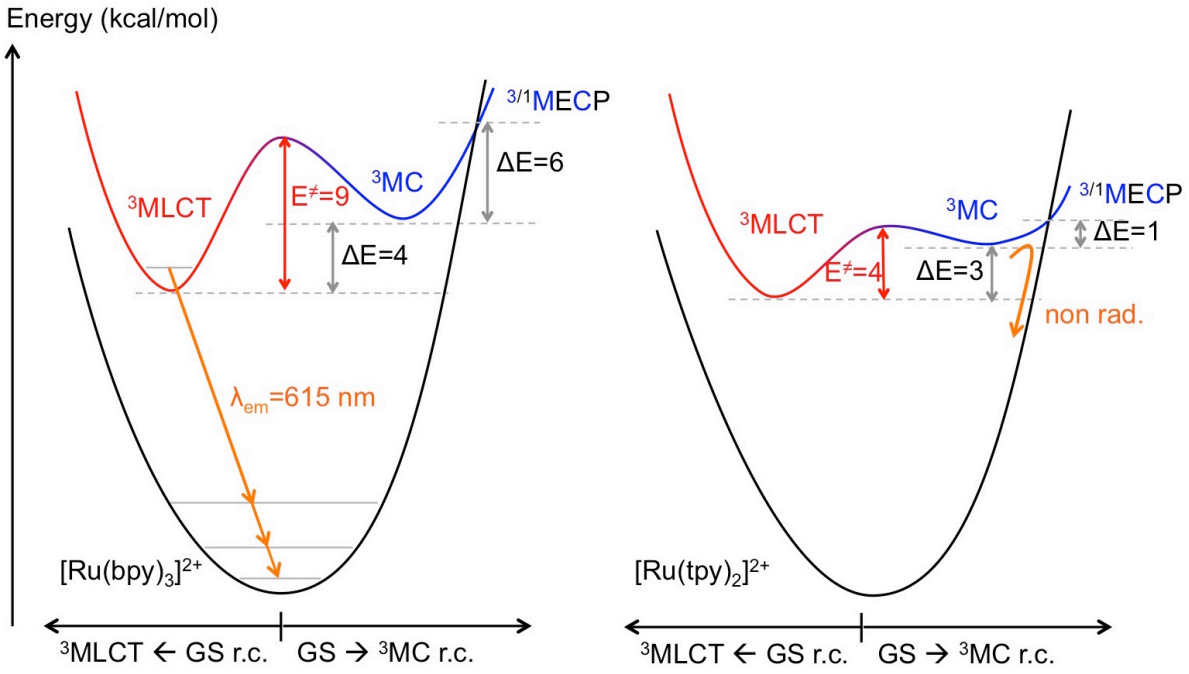

Scheme 1: Potential energy curves computed for $[Ru(bpy)_3]^{2+}$ (left) and $[Ru(tpy)_2]^{2+}$ (right) [45].

Having validated the methods and having gained a significant experience of their use on coordination compounds in their ground and excited states, we have embarked on applying them to more challenging projects involving photoinduced ligand release. This has enabled us to develop strategies for their systematic use to map the topology of both the singlet and triplet PES as a highly convenient alternative to relaxed surface scan approaches.

3. Photorelease of a monodentate ligand

Photoactivated chemotherapy involves the light-induced breaking of a chemical bond that releases at least one biologically active fragment. The goal of realising effective and applicable photoactivated chemotherapeutic complexes has therefore driven significant experimental efforts for the investigation of ligand release photochemistry. In the course of their studies on the photorelease of thioether ligands from Ru(II) complexes, Bonnet *et al.* obtained strikingly different photosubstitution yields (φ(photosub.)) depending on the bidentate ligand that was bound to the metal, ranging from 2% to an impressive 30% (Scheme 2) [66]. The method by which the photosubstitution yields were estimated is reported in the original publication [66]. Theoretical studies were subsequently undertaken to rationalize this behaviour.

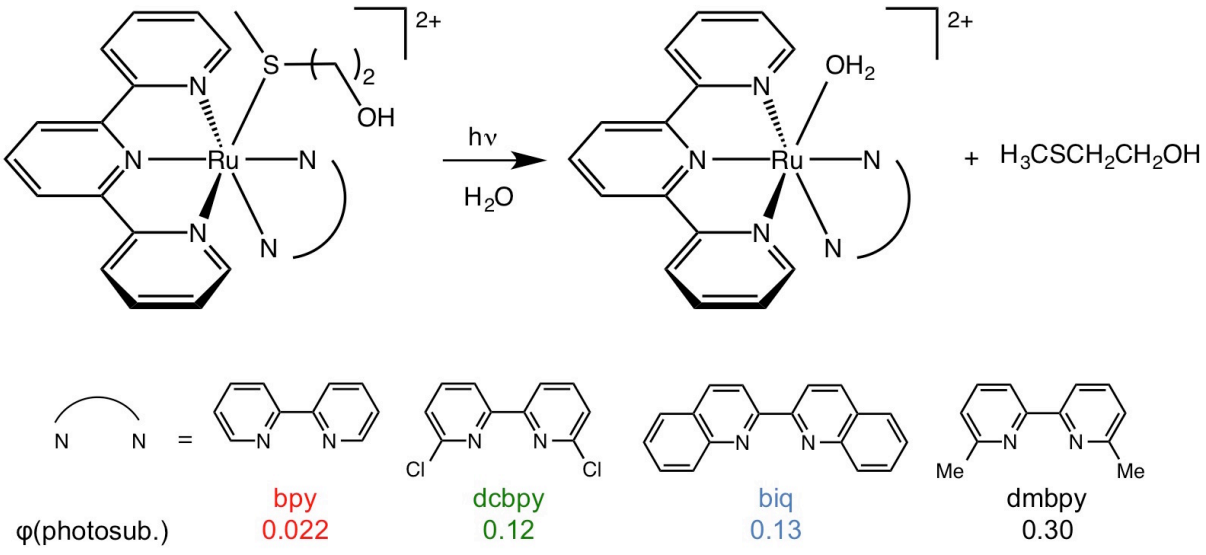

Scheme 2: Monodentate thioether photosubstitution yields φ(photosub.) [66].

An intuitive approximation of the reaction coordinate involved in the release of a monodentate ligand is the distance between the metal and the initally bound/eventually unbound atom. From the practical point of view of a theoretician, this distance is a natural parameter to be scanned in a relaxed surface scan [23][30][33][36]. We have performed geometry optimizations followed by NEB minimum energy path calculations and transition state optimizations on the four complexes shown in Scheme 2. These calculations point to the fact that two local minima could be located in the ^{3}MC region, both displaying major elongations towards the thioether ligand but to various degrees. Indeed, for dcbpy and biq, which display intermediate photosubstitution yields, a ^{3}MC state with a closely associated thioether ligand (Ru-S≈3 Å) was obtained, called $^3MC_{hexa}$, as well as a ^{3}MC state with a significantly extended Ru-S distance of ~4 Å, called $^3MC_{penta}$. The $^3MC_{hexa}$-$^3MC_{penta}$ internal conversion process is slightly downhill and its activation energy is minimal, less than 3 kcal/mol. For bpy, which displays the lowest φ(photosub.), only $^3MC_{hexa}$ was obtained. On the contrary, for dmbpy, which displays the highest φ(photosub.), only $^3MC_{penta}$ could be located. This combination of factors has led us to propose the following mechanistic hypothesis: $^3MC_{hexa}$ with a shorter Ru-S distance would be prone to geminate recombination through the associated $^{3/1}$MECP that leads the system back to the reactant ground state; on the other hand, $^3MC_{penta}$ with a far longer Ru-S distance would be prone to ligand dissociation, following diffusion of its weakly bound thioether ligand, which in turn would lead towards the photoproduct through solvent trapping (Scheme 3) [67]. This therefore explains the highly differing photochemical ligand ejection efficiencies displayed by the bpy and dmbpy complexes. Further, the intermediate efficiencies of the dcbpy and biq complexes can then be rationalised by the population of $^3MC_{penta}$ necessitating transient population of $^3MC_{hexa}$, with its associated potential leak towards reactant.

Coord. Chem. Rev. 2020, 408, 213184.
https://doi.org/10.1016/j.ccr.2020.213184

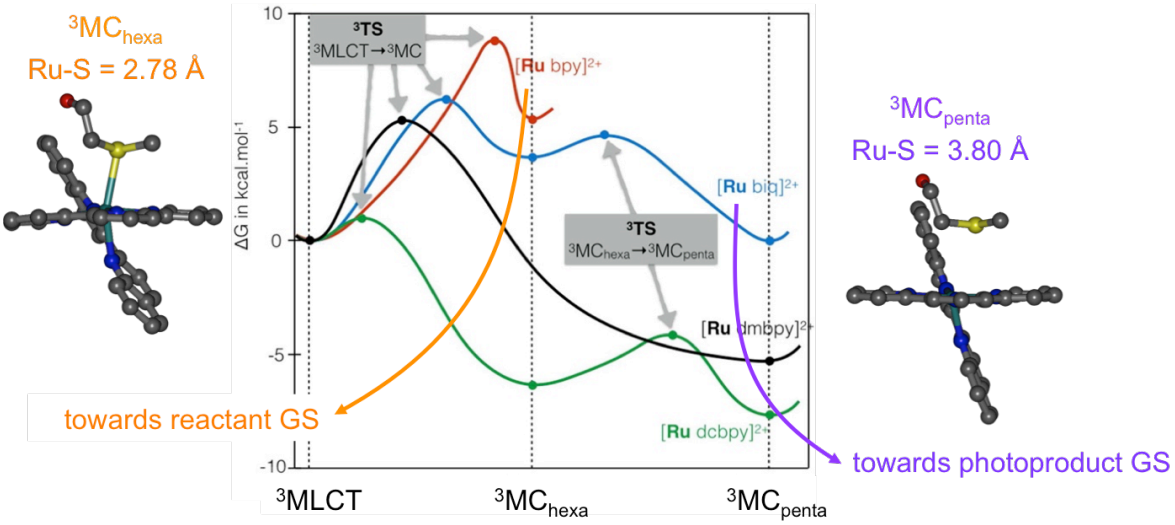

***Scheme 3**: Triplet free energy profiles for the bpy (red), dcbpy (green), biq (blue) and dmbpy (black) complexes in water at 298 K (^{3}MLCT states aligned for comparison purposes). The preferential roles assigned to $^3MC_{hexa}$ (geminate recombination towards starting material, orange arrow) and $^3MC_{penta}$ (evolution towards photoproduct, purple arrow) are schematized through crossings with the relevant singlet PES. Illustration with the biq ligand showing the chemical structure and Ru-S distance in the ^{3}MC states proposed to play two distinct roles [67].*

4. Photorelease of a bidentate ligand

Although the most common photolabilized ligands are monodentate ([17][18] and references therein), there are a few examples where bidentate ligands such as diimines [68][69][70][71] or aminoacids [72] have been photoreleased, or 'photouncaged' in the jargon, from Ru(II) complexes, to reveal their biological activity. Alternatively the photoejection of bidentate ligands has been used as an efficient trigger for molecular machines [73][74][75][76][50].

Experimental work in the Elliott group has largely focussed on the photophysical properties of complexes of 1,2,3-triazole-based ligands as analogues for more conventional polypyridyl ligand systems [77]. Whilst these ligand systems have proved enormously versatile the preparation of complexes for luminescent applications [78], they have also offered significant and unique insights into photoreactive excited state processes. During the course of our investigations in this field, we designed a series of complexes containing various proportions of bpy and btz ligands (btz = 1,1'-dibenzyl-4,4'-bi-1,2,3-triazolyl) [79] with the aim of gradually narrowing the energy gap from the bpy-localised ^{3}MLCT state to the potentially dissociative ^{3}MC states in order to favour ligand photorelease with increasing btz content [77].

Coord. Chem. Rev. 2020, 408, 213184.
https://doi.org/10.1016/j.ccr.2020.213184

Indeed, both the heteroleptic complexes $[Ru(bpy)_2(btz)]^{2+}$ and $[Ru(bpy)(btz)_2]^{2+}$ prove to be photochemically reactive with release of a btz ligand in donor solvents [80][81]. Whilst $[Ru(bpy)_2(btz)]^{2+}$ releases btz in acetonitrile to form *cis*-$[Ru(bpy)_2(NCMe)_2]^{2+}$ in a similar manner to that observed for other Ru(II) complexes (e.g. $[Ru(bpy)_2(dmbpy)]^{2+}$ [68]), the alternative heteroleptic complex $[Ru(bpy)(btz)_2]^{2+}$ displays highly novel photochemical behaviour; during the process of release of one of the btz ligands the retained bidentate ligands undergo rearrangement such that they become coplanar in the photoproduct *trans*-$[Ru(bpy)(btz)(NCMe)_2]^{2+}$ (Scheme 4). Significantly, this proceeds with observation of an intermediate photoproduct in which one btz ligand is coordinated in the monodentate fashion and which shows a high degree of stability. Remarkably, this allowed us to crystallize and structurally characterise the intermediate photoproduct (Figure 4) [80].

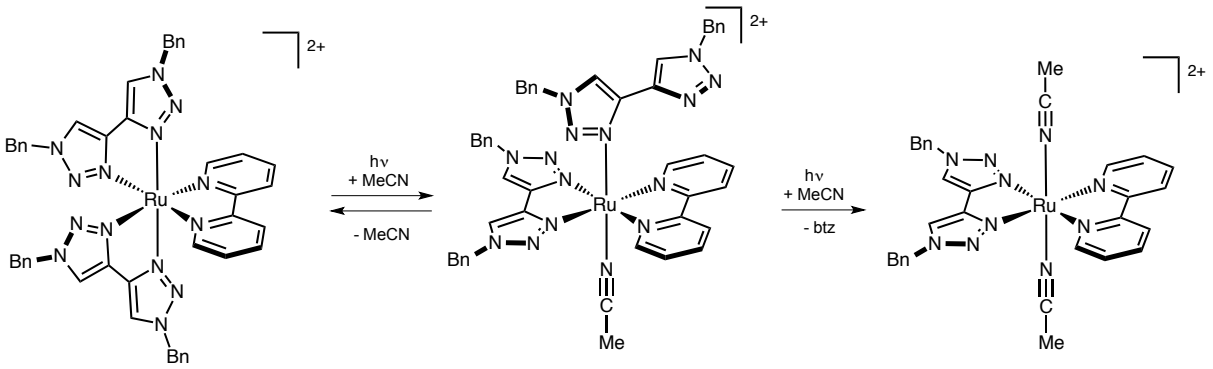

Scheme 4. Two-step photochemical reactivity of $[Ru(bpy)(btz)_2]^{2+}$ in acetonitrile, involving two successive one-photon absorptions .

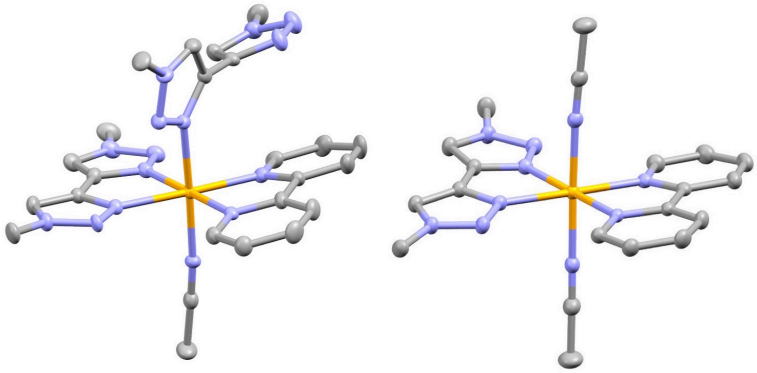

Coord. Chem. Rev. 2020, 408, 213184.
https://doi.org/10.1016/j.ccr.2020.213184

Figure 4: ORTEP diagrams of the intermediate photoproduct trans-[Ru(bpy)(κ²-btz)(κ¹-btz)(NCMe)]²⁺ (left) and of the final photoproduct trans-[Ru(bpy)(btz)(NCMe)₂]²⁺ (right) (phenyl groups of the benzyl substituents of the triazole rings have been removed for clarity; H atoms and counterions not shown) *[80]*

From a mechanistic point of view, the isolation and structural characterization of a complex bearing a monodentate btz ligand *trans* to the incoming MeCN ligand unambiguously demonstrated the existence of κ^1 half-bound bidentate ligand complexes that had long been postulated in solution for this and other systems leading to *cis* photoproducts [82][83][84][85]. We then had in hand the experimental evidence of a stepwise process requiring two separate one-photon absorptions, taking place under continuous irradiation in acetonitrile, the second step requiring much longer irradiation times than the first one [86]. Theoretical mechanistic investigations initially involved the determination of ^{3}MLCT and axially elongated ^{3}MC minima (inspired by the geometric parameters for the ^{3}MC state described earlier for $[Ru(bpy)_3]^{2+}$) and relaxed surface scans between these states (although the definition of the reaction coordinate is not as trivial as with a monodentate ligand). These scans allowed us to identify a previously unreported ^{3}MC local minimum repelling a *single* bidentate ligand through the elongation of two *cis* Ru-N bonds, which thus seemed a much better candidate for btz release than classical MC states displaying two *trans* elongations towards two *different* ligands (Figure 5). In addition this new type of ^{3}MC state displays a flattened geometry in relation to the widening of the angle between the two unrepelled ligands and thus approaching the coplanar arrangement observed in the photoproducts [87].

Coord. Chem. Rev. 2020, 408, 213184.
https://doi.org/10.1016/j.ccr.2020.213184

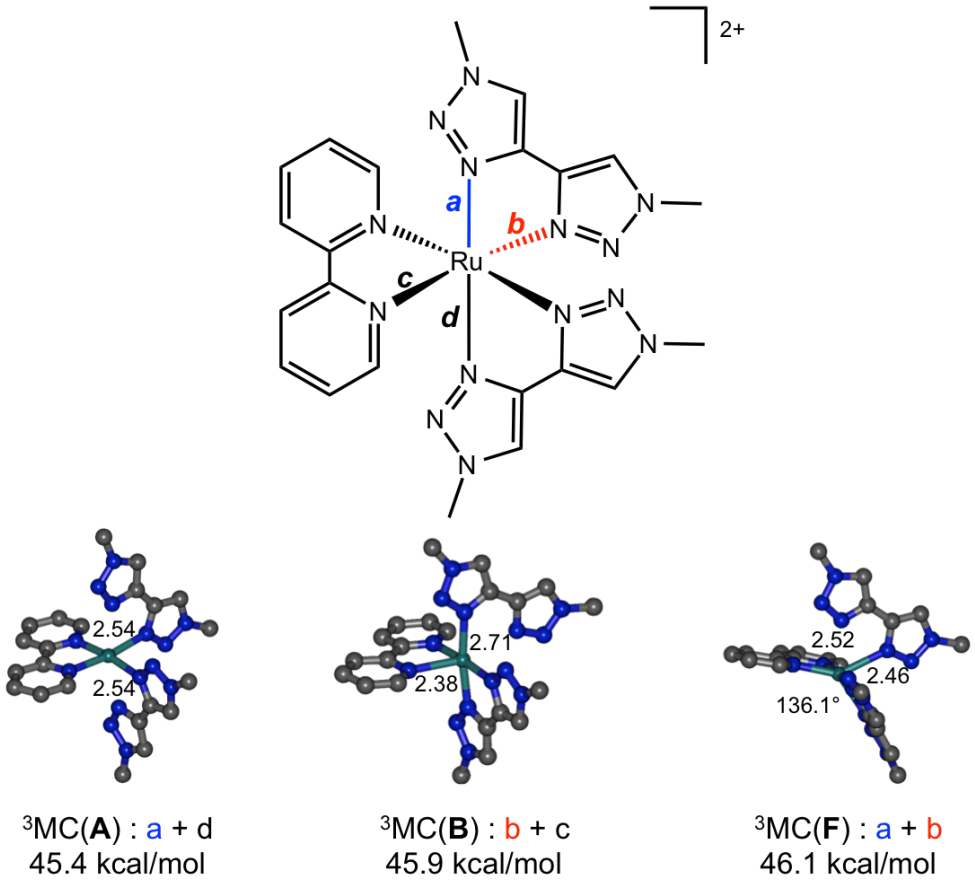

Figure 5: Examples of classical (trans-elongated, A/B) and flattened (cis-elongated, F) ^{3}MC minima with remarkable distances along the most elongated bonds (a+d, b+c or a+b) and angles. Electronic energies with respect to that of the ground state [87].

Once flattened *cis*-elongated ^{3}MC(**F**) states are populated, and given the fact that we know, from the crystal structure of the intermediate photoproduct, that the two unrepelled ligands will eventually become coplanar, we were able to build a guess geometry and subsequently optimize another local ^{3}MC minimum bearing this approximate coplanarity, shown as ^{3}MC(**P**) on Figure 6. Here the '**P**' stands for pentacoordinate as one of the Ru-N distances has significantly increased to 3.2 Å and the ligand can therefore be considered to have formally undergone dechelation.

Minimum energy crossing points were located for the hexacoordinate ^{3}MC(**A/B/F**) states which were found to connect to the ^{1}PES of the reactant complex in a similar manner to the ^{3}MC state of $[Ru(bpy)_3]^{2+}$ and the $^3MC_{hexa}$ states of the $[Ru(tpy)(diimine)(thioether)]^{2+}$ series (*vide supra*). However, in the neighbourhood of ^{3}MC(**P**) state lies a crucial minimum energy crossing point, very clearly mentioned in theoretical works by Vanquickenborne and Ceulemans [88], that leads the system to the ground state PES of a pentacoordinate,

electrophilic, 16-electron coordinatively unsaturated species. Singlet geometry optimization from $^{3/1}$MECP(**P**) results in a shortening of the Ru-N bond to the κ^1-btz ligand and full relaxation to a square pyramid GS(**P**) displaying a bare face with a vacancy available for nucleophilic attack by the entering ligand on the face opposite to the κ^1-btz ligand, thus leading to the *trans* intermediate photoproduct shown on Scheme 4. Note that pentacoordinate intermediates have also been described in the framework of photoreactivity studies on iron [89][90] or chromium [91] complexes.

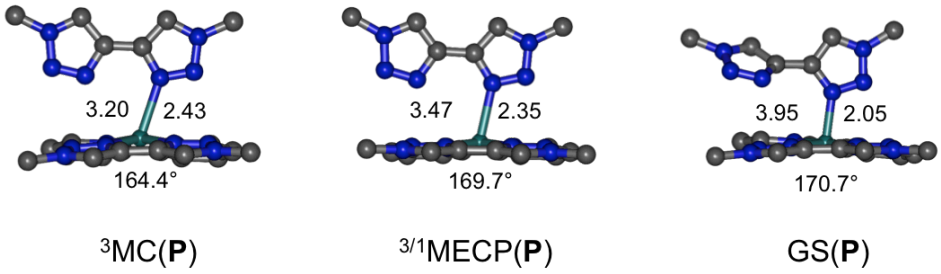

Figure 6: Examples of pentacoordinate ^{3}MC state, $^{3/1}$MECP and singlet ground state with key Ru-N distances and smallest trans N-Ru-N angles of the approximate square-plane [87].

In this project, a combination of geometry optimizations, relaxed surface scans and NEB calculations to connect all triplet states has enabled us to propose a full reaction mechanism for the formation of the *trans* intermediate photoproduct.

5. Generalization: a return to $Ru(bpy)_3^{2+}$

From the early 1970s $[Ru(bpy)_3]^{2+}$ has been intensively studied for the luminescent and electron and energy transfer properties of its long-lived ^{3}MLCT excited state [92]. Meanwhile, its photostability was challenged in the presence of coordinating anions such as SCN^- [93] and Cl^- [82] to form $Ru(bpy)_2X_2$ photoproducts following the loss of one bpy ligand, thus involving some dissociative excited state that is presumably of metal-centred character. The population of ^{3}MC states could be enhanced under high laser power excitation in water [85], although the dominant excited state decay route remained reformation of starting material $[Ru(bpy)_3]Cl_2$. Under more classical excitation conditions, Hauser and coworkers did not observe population of the ^{3}MC state of $[Ru(bpy)_3](PF_6)_2$, whether by ultrafast transient absorption spectroscopy following excitation in CH_3CN at 400 nm [94] or by TR-IR in

CD_3CN or KBr pellets [59]. On the other hand, using excitation at the same wavelength but in dichloromethane solution, Onda *et al.* reported the observation of the transient ^{3}MC state of $[Ru(bpy)_3]Cl_2$ and based their reasoning on the 1600 cm^{-1} region of the TR-IR spectrum [95][96]. All in all, the observation of relatively inefficient photoreactivity of $[Ru(bpy)_3]^{2+}$, but only under certain conditions, and the glimpsed spectroscopic characterization of its ^{3}MC state (or lack of characterization) illustrate the complexity of this case and requirement for further investigations.

Having identified new ^{3}MC states displaying peculiar flattened geometries with one single bidentate btz ligand repelled for $[Ru(bpy)(btz)_2]^{2+}$ [87], we embarked on a search for similar structures on the ^{3}PES for $[Ru(bpy)_3]^{2+}$ itself. With a suitable guess geometry based on the identified key structural parameters we indeed found that a similar flattened ^{3}MC state is also a local minimum for this archetypal complex. In this novel state, which we call $^3MC_{cis}$ (due to the elongation of two mutually *cis* Ru-N bonds), the highest singly occupied molecular orbital is $d_{x^2-y^2}$-like, whereas it is d_{z^2}-like in the now 'classical' ^{3}MC state identified earlier in Section 2, which we now call here $^3MC_{trans}$ (as it displays two elongated *trans* Ru-N bonds, Figure 7). In this new nomenclature the Ru(II) btz states shown on Figure 5 ^{3}MC(**A**/**B**) are of the $^3MC_{trans}$ type, while the flattened ^{3}MC(**F**) state is of the $^3MC_{cis}$ type.

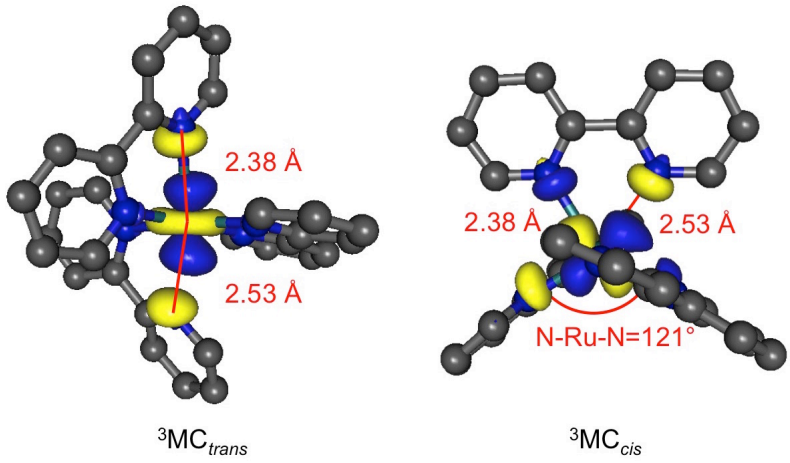

Figure 7. Classical trans-elongated $^3MC_{trans}$ state and novel cis-elongated $^3MC_{cis}$ state of $[Ru(bpy)_3]^{2+}$ with most significant Ru-N elongations and their SOMO+1 [97].

Both states are only 2 kcal/mol apart, and the conversion from one to the other is essentially barrierless (Scheme 5) [97]. In addition, the activation energy to populate them from the lowest ^{3}MLCT state is similar (9 kcal/mol for $^3MC_{trans}$ vs 10 kcal/mol for $^3MC_{cis}$), which means that both ^{3}MC states are likely to be populated. At this stage it might be tempting to assign a preferential role of phosphorescence quencher to the classical $^3MC_{trans}$, while the novel $^3MC_{cis}$ would be more prone to photoreactivity and particularly bpy loss. However, what one can also note with confidence at this stage is the observation that the $^{3/1}$MECP for the newly identified $^3MC_{cis}$ state lies 3 kcal/mol lower in energy than that for the established $^3MC_{trans}$ state and thus this previously unknown ^{3}MC state will inevitably play a prominent role in the *photophysics* of this most famous of chemical compound. We are currently actively working on exploring the *photochemical* fate of these two distinct ^{3}MC states and will report these results elsewhere in due course.

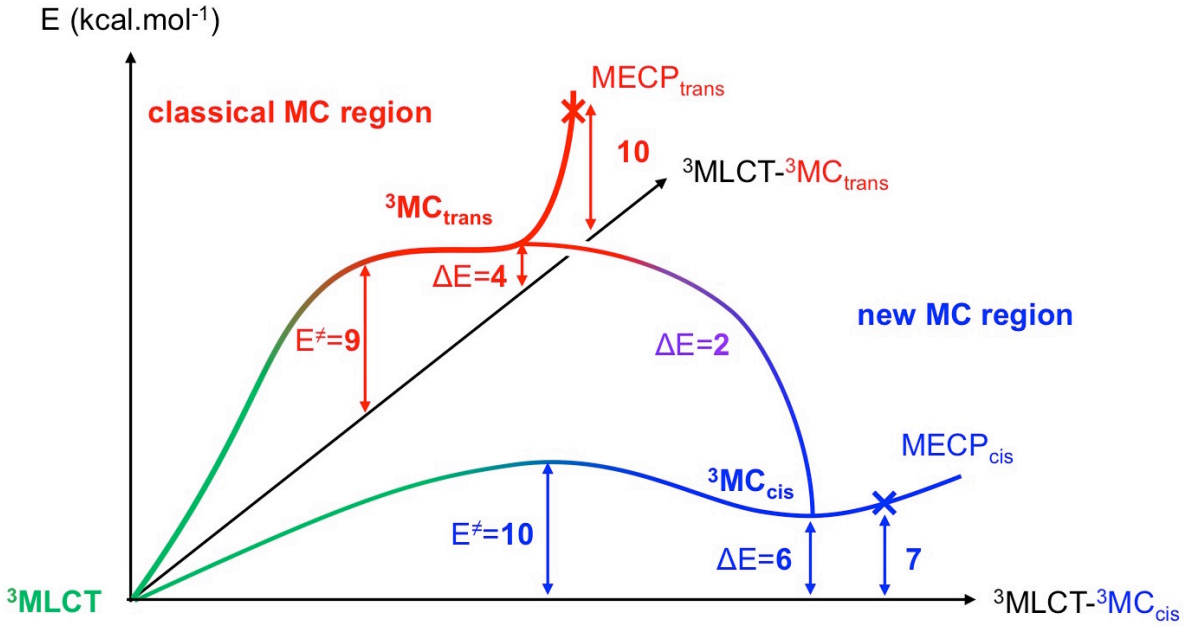

Scheme 5: Minimum energy paths, energy barriers and energy gaps for the ^{3}MLCT-$^3MC_{trans}$, ^{3}MLCT-$^3MC_{cis}$ and $^3MC_{trans}$-$^3MC_{cis}$ internal conversions of $[Ru(bpy)_3]^{2+}$ [97].

6. Conclusions and Outlook

Over recent years our joint projects and the combination of our synthetic, spectroscopic and theoretical skills have led us to discover most exciting and intriguing features regarding triplet

excited states of Ru(II) complexes. '*The ^{3}MC state*', a denomination that pervades the literature, actually covers an expansive region of the ^{3}PES displaying several local minima to which we tentatively assign preferential roles as photophysics and photochemistry quenchers and/or promoters.

Our recent work has identifed highly novel flattened ^{3}MC states as being intimately involved in *trans* photoproduct formation. In fact, looking back on one of our previous studies on photoisomerization mechanisms, flattened ^{3}MC states had made an appearance but we did not appreciate their full significance at the time [55]. Having then found some in $[Ru(bpy)_3]^{2+}$ itself, such distorted states seem to be a common feature in Ru(II) coordination compounds, and possibly in coordination chemistry in general since flattened MC states have been recently described for other metals (Fe [98], Ir [99][100][101]) as well as for the *cis*-*trans* isomerization of $[Ru(bpy)_2(PMe_3)(OH_2)]^{2+}$ [102]. We have recently reported the remarkable and unprecedented photochemical reactivity of the Os(II) complex $[Os(btz)_3]^{2+}$, which in acetonitrile yields both *cis* and *trans* isomers of the photoproduct $[Os(btz)_2(NCMe)_2]^{2+}$ with observation of both *cis* and *trans* ligand-loss intermediates $[Os(\kappa^2\text{-btz})_2(\kappa^1\text{-btz})(NCMe)]^{2+}$ [103]. Clearly, the *trans* photoproduct formation pathway for this Os(II) complex should also involve flattened $^3MC_{cis}$- and ^{3}MC(**P**)-like states.

What our results reveal is the importance of not only identifying *all* possible ^{3}MC states on the ^{3}PES of a given complex as well as their relative accessibility from the ^{3}MLCT state, but also the minimum energy paths that connect them to each other and the relative accessibility of minimum energy crossing points to singlet ground state surfaces of both the reactant and photoproducts (Scheme 6). A further step would be to investigate the preferential relaxation paths of the systems by excited state dynamics, as only certain specific ^{3}MC states are productive towards ligand loss. This additional knowledge and understanding enables a far deeper rationalisation of experimental observations and microscopic mechanisms, but will also provide predictive tools which will give the synthetic chemist the ability to confidently control and fine tune photochemical behaviour with the aim of influencing selective ^{3}MC population to achieve efficient photorelease.

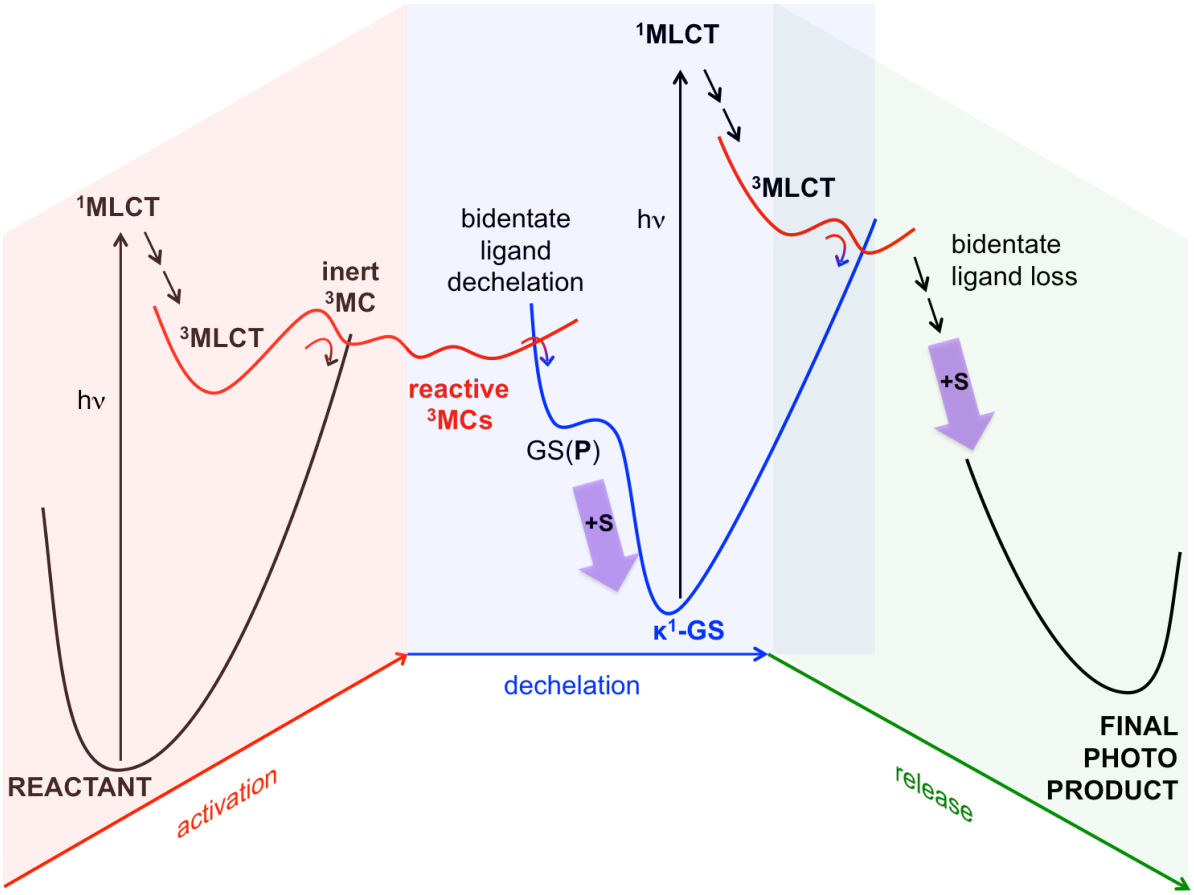

Scheme 6: Our current schematic view of the elementary steps and intermediate states populated along the photoinduced release of a bidentate ligand towards the formation of a given final photoproduct. The purple arrows represent solvent capture (S = solvent). In the case of multiple photoproducts (eg cis and trans isomers), additional states and bifurcations should be involved. For the sake of clarity, only selected interconversions are shown.

No doubt the refined view that we currently have of the ^{3}PES topology will soon have to be updated. The photochemical transformations observed in Ru(II) bis(bitriazolyl) complexes, for example, has led to enlightening insights on possible processes operating on the lowest ^{3}PES. Beyond these immediate systems this has led to further fundamental insights of much broader significance in other very well-known systems. Whilst mechanistic details for the formation of the *trans* intermediate κ^1-GS photoproduct from tris-chelate complexes have been elucidated [87], the equivalent details regarding the far more common formation of *cis* photoproducts from chelate ligand release have yet to fully determined and are the subject of ongoing research in our laboratories. In this regard we can expect great insights from the improved theoretical methods described here combined with ultrafast spectroscopies, particularly the most recent developments of ultrafast time-resolved X-ray spectroscopies [104][105][106] enabled by free electron lasers.

Acknowledgements

We thank the French Ministry for Higher Education and Research for a Ph.D. fellowship to A.S. The French contribution to this work was performed using HPC resources from CALMIP (Grant 2018-[p1112]). Some of the work in the Elliott group covered in this review involved use of computational resources via his membership of the UK's HEC Materials Chemistry Consortium, which is funded by EPSRC (EP/L000202, EP/R029431), and we therefore wish to acknowledge the ARCHER UK National Supercomputing Service (http://www.archer.ac.uk).

Supporting information

Animations along the ^{3}MLCT-^{3}MC minimum energy path for $[Ru(bpy)_3]^{2+}$: geometries, highest SOMO (dπ) and SOMO+1 (π* followed by dσ*).

References

[1] C. Mari, V. Pierroz, S. Ferrari, G. Gasser, Combination of Ru(II) complexes and light: new frontiers in cancer therapy, Chem. Sci. 6 (2015) 2660–2686. https://doi.org/10.1039/C4SC03759F.

[2] F. Heinemann, J. Karges, G. Gasser, Critical Overview of the Use of Ru(II) Polypyridyl Complexes as Photosensitizers in One-Photon and Two-Photon Photodynamic Therapy, Acc. Chem. Res. 50 (2017) 2727–2736. https://doi.org/10.1021/acs.accounts.7b00180.

[3] G. Lemercier, M. Four, S. Chevreux, Two-photon absorption properties of 1,10-phenanthroline-based Ru(II) complexes and related functionalized nanoparticles for potential application in two-photon excitation photodynamic therapy and optical power limiting, Coord. Chem. Rev. 368 (2018) 1–12. https://doi.org/10.1016/j.ccr.2018.03.019.

[4] J. Liu, C. Zhang, T.W. Rees, L. Ke, L. Ji, H. Chao, Harnessing ruthenium(II) as photodynamic agents: Encouraging advances in cancer therapy, Coord. Chem. Rev. 363 (2018) 17–28. https://doi.org/10.1016/j.ccr.2018.03.002.

[5] C.K. Prier, D.A. Rankic, D.W.C. MacMillan, Visible Light Photoredox Catalysis with Transition Metal Complexes: Applications in Organic Synthesis, Chem. Rev. 113 (2013) 5322–5363. https://doi.org/10.1021/cr300503r.

[6] M.H. Shaw, J. Twilton, D.W.C. MacMillan, Photoredox Catalysis in Organic Chemistry, J. Org. Chem. 81 (2016) 6898–6926. https://doi.org/10.1021/acs.joc.6b01449.

[7] J. Twilton, C. (Chip) Le, P. Zhang, M.H. Shaw, R.W. Evans, D.W.C. MacMillan, The

merger of transition metal and photocatalysis, Nat. Rev. Chem. 1 (2017) 0052. https://doi.org/10.1038/s41570-017-0052.

[8] M.R. Gill, J. Garcia-Lara, S.J. Foster, C. Smythe, G. Battaglia, J.A. Thomas, A ruthenium(II) polypyridyl complex for direct imaging of DNA structure in living cells, Nat. Chem. 1 (2009) 662–667. https://doi.org/10.1038/nchem.406.

[9] B. Pashaei, H. Shahroosvand, M. Graetzel, M.K. Nazeeruddin, Influence of Ancillary Ligands in Dye-Sensitized Solar Cells, Chem. Rev. 116 (2016) 9485–9564. https://doi.org/10.1021/acs.chemrev.5b00621.

[10] C. Daniel, C. Gourlaouen, Chemical bonding alteration upon electronic excitation in transition metal complexes, Coord. Chem. Rev. 344 (2017) 131–149. https://doi.org/10.1016/j.ccr.2016.10.010.

[11] W.M. Wallace, P.E. Hoggard, A Simple Photochemical Synthesis of Some Bis(bipyridyl)ruthenium(II) Complexes, Inorg. Chem. 18 (1979) 2934–2935.

[12] B. Durham, J.L. Walsh, C.L. Carter, T.J. Meyer, Synthetic Applications of Photosubstitution Reactions of Poly(pyridyl) Complexes of Ruthenium(II), Inorg. Chem. 19 (1980) 860–865.

[13] D.V. Pinnick, B. Durham, Photosubstitution Reactions of $Ru(bpy)_2XY^{n+}$ Complexes, Inorg. Chem. 23 (1984) 1440–1445.

[14] C.R. Hecker, P.E. Fanwick, D.R. McMillin, Evidence for Dissociative Photosubstitution Reactions of $[Ru(trpy)(bpy)(NCCH_3)]^{2+}$. Crystal and Molecular Structure of $[Ru(trpy)(bpy)(py)](PF_6)_2.(CH_3)_2CO$, Inorg. Chem. 30 (1991) 659–666.

[15] P.C. Ford, Metal complex strategies for photo-uncaging the small molecule bioregulators nitric oxide and carbon monoxide, Coord. Chem. Rev. 376 (2018) 548–564. https://doi.org/10.1016/j.ccr.2018.07.018.

[16] J.K. White, R.H. Schmehl, C. Turro, An overview of photosubstitution reactions of Ru(II) imine complexes and their application in photobiology and photodynamic therapy, Inorganica Chim. Acta. 454 (2017) 7–20. https://doi.org/10.1016/j.ica.2016.06.007.

[17] A. Li, C. Turro, J.J. Kodanko, Ru(II) polypyridyl complexes as photocages for bioactive compounds containing nitriles and aromatic heterocycles, Chem. Commun. 54 (2018) 1280–1290. https://doi.org/10.1039/C7CC09000E.

[18] A. Li, C. Turro, J.J. Kodanko, Ru(II) Polypyridyl Complexes Derived from Tetradentate Ancillary Ligands for Effective Photocaging, Acc. Chem. Res. 51 (2018) 1415–1421. https://doi.org/10.1021/acs.accounts.8b00066.

[19] S. Bonnet, Why develop photoactivated chemotherapy?, Dalton Trans. 47 (2018) 10330–10343. https://doi.org/10.1039/C8DT01585F.

[20] B. Colasson, A. Credi, G. Ragazzon, Light-driven molecular machines based on ruthenium(II) polypyridine complexes: Strategies and recent advances, Coord. Chem. Rev. 325 (2016) 125–134. https://doi.org/10.1016/j.ccr.2016.02.012.

[21] A. Gabrielsson, S. Záliš, P. Matousek, M. Towrie, A. Vlček, Ultrafast Photochemical Dissociation of an Equatorial CO Ligand from *trans(X,X)*-$[Ru(X)_2(CO)_2(bpy)]$ (X = Cl, Br, I):

A Picosecond Time-Resolved Infrared Spectroscopic and DFT Computational Study, Inorg. Chem. 43 (2004) 7380–7388. https://doi.org/10.1021/ic049548n.

[22] A. Petroni, L.D. Slep, R. Etchenique, Ruthenium(II) 2,2'-Bipyridyl Tetrakis Acetonitrile Undergoes Selective Axial Photocleavage, Inorg. Chem. 47 (2008) 951–956. https://doi.org/10.1021/ic7018204.

[23] L. Salassa, C. Garino, G. Salassa, R. Gobetto, C. Nervi, Mechanism of Ligand Photodissociation in Photoactivable $[Ru(bpy)_2L_2]^{2+}$ Complexes: A Density Functional Theory Study, J. Am. Chem. Soc. 130 (2008) 9590–9597. https://doi.org/10.1021/ja8025906.

[24] Y. Liu, D.B. Turner, T.N. Singh, A.M. Angeles-Boza, A. Chouai, K.R. Dunbar, C. Turro, Ultrafast Ligand Exchange: Detection of a Pentacoordinate Ru(II) Intermediate and Product Formation, J. Am. Chem. Soc. 131 (2009) 26–27. https://doi.org/10.1021/ja806860w.

[25] L. Salassa, C. Garino, G. Salassa, C. Nervi, R. Gobetto, C. Lamberti, D. Gianolio, R. Bizzarri, P.J. Sadler, Ligand-Selective Photodissociation from $[Ru(bpy)(4AP)_4]^{2+}$: a Spectroscopic and Computational Study, Inorg. Chem. 48 (2009) 1469–1481. https://doi.org/10.1021/ic8015436.

[26] L. Salassa, E. Borfecchia, T. Ruiu, C. Garino, D. Gianolio, R. Gobetto, P.J. Sadler, M. Cammarata, M. Wulff, C. Lamberti, Photo-Induced Pyridine Substitution in *cis*-$[Ru(bpy)_2(py)_2]Cl_2$: A Snapshot by Time-Resolved X-ray Solution Scattering, Inorg. Chem. 49 (2010) 11240–11248. https://doi.org/10.1021/ic102021k.

[27] E. Borfecchia, C. Garino, D. Gianolio, L. Salassa, R. Gobetto, C. Lamberti, Monitoring excited state dynamics in *cis*-$[Ru(bpy)_2(py)_2]^{2+}$ by ultrafast synchrotron techniques, Catal. Today. 229 (2014) 34–45. https://doi.org/10.1016/j.cattod.2013.11.057.

[28] L. Ding, L.W. Chung, K. Morokuma, Excited-State Proton Transfer Controls Irreversibility of Photoisomerization in Mononuclear Ruthenium(II) Monoaquo Complexes: A DFT Study, J. Chem. Theory Comput. 10 (2014) 668–675. https://doi.org/10.1021/ct400982r.

[29] S.E. Greenough, G.M. Roberts, N.A. Smith, M.D. Horbury, R.G. McKinlay, J.M. Żurek, M.J. Paterson, P.J. Sadler, V.G. Stavros, Ultrafast photo-induced ligand solvolysis of cis-$[Ru(bipyridine)_2(nicotinamide)_2]^{2+}$: experimental and theoretical insight into its photoactivation mechanism, Phys Chem Chem Phys. 16 (2014) 19141–19155. https://doi.org/10.1039/C4CP02359E.

[30] M.R. Camilo, C.R. Cardoso, R.M. Carlos, A.B.P. Lever, Photosolvolysis of *cis*-$[Ru(\alpha\text{-diimine})_2(4\text{-aminopyridine})_2]^{2+}$ Complexes: Photophysical, Spectroscopic, and Density Functional Theory Analysis, Inorg. Chem. 53 (2014) 3694–3708. https://doi.org/10.1021/ic5000205.

[31] E. Wachter, E.C. Glazer, Mechanistic Study on the Photochemical "Light Switch" Behavior of $[Ru(bpy)_2dmdppz]^{2+}$, J. Phys. Chem. A. 118 (2014) 10474–10486. https://doi.org/10.1021/jp504249a.

[32] T.A. Word, C.L. Whittington, A. Karolak, M.T. Kemp, H.L. Woodcock, A. van der Vaart, R.W. Larsen, Photoacoustic calorimetry study of ligand photorelease from the Ru(II)bis(2,2′-bipyridine)(6,6′-dimethyl-2,2′-bipyridine) complex in aqueous solution, Chem. Phys. Lett. 619 (2015) 214–218. https://doi.org/10.1016/j.cplett.2014.11.012.

[33] Y.-J. Tu, S. Mazumder, J.F. Endicott, C. Turro, J.J. Kodanko, H.B. Schlegel, Selective Photodissociation of Acetonitrile Ligands in Ruthenium Polypyridyl Complexes Studied by Density Functional Theory, Inorg. Chem. 54 (2015) 8003–8011. https://doi.org/10.1021/acs.inorgchem.5b01202.

[34] P.A. Scattergood, U. Khushnood, A. Tariq, D.J. Cooke, C.R. Rice, P.I.P. Elliott, Photochemistry of $[Ru(pytz)(btz)_2]^{2+}$ and Characterization of a κ^1-btz Ligand-Loss Intermediate, Inorg. Chem. 55 (2016) 7787–7796. https://doi.org/10.1021/acs.inorgchem.6b00782.

[35] M. Kubeil, R.R. Vernooij, C. Kubeil, B.R. Wood, B. Graham, H. Stephan, L. Spiccia, Studies of Carbon Monoxide Release from Ruthenium(II) Bipyridine Carbonyl Complexes upon UV-Light Exposure, Inorg. Chem. 56 (2017) 5941–5952. https://doi.org/10.1021/acs.inorgchem.7b00599.

[36] K. Nisbett, Y.-J. Tu, C. Turro, J.J. Kodanko, H.B. Schlegel, DFT Investigation of Ligand Photodissociation in $[Ru(II)(tpy)(bpy)(py)]^{2+}$ and $[Ru(II)(tpy)(Me_2bpy)(py)]^{2+}$ Complexes, Inorg. Chem. 57 (2018) 231–240. https://doi.org/10.1021/acs.inorgchem.7b02398.

[37] A.J. Orr-Ewing, Taking the plunge: chemical reaction dynamics in liquids, Chem. Soc. Rev. 46 (2017) 7597–7614. https://doi.org/10.1039/C7CS00331E.

[38] M.R.A. Blomberg, T. Borowski, F. Himo, R.-Z. Liao, P.E.M. Siegbahn, Quantum Chemical Studies of Mechanisms for Metalloenzymes, Chem. Rev. 114 (2014) 3601–3658.

[39] C.M. Marian, Spin-orbit coupling and intersystem crossing in molecules: Spin-orbit coupling, Wiley Interdiscip. Rev. Comput. Mol. Sci. 2 (2012) 187–203. https://doi.org/10.1002/wcms.83.

[40] T.J. Penfold, E. Gindensperger, C. Daniel, C.M. Marian, Spin-Vibronic Mechanism for Intersystem Crossing, Chem. Rev. 118 (2018) 6975–7025. https://doi.org/10.1021/acs.chemrev.7b00617.

[41] N.H. Damrauer, G. Cerullo, A. Yeh, T.R. Boussie, C.V. Shank, J.K. McCusker, Femtosecond Dynamics of Excited-State Evolution in $[Ru(bpy)_3]^{2+}$, Science. 275 (1997) 54–57. https://doi.org/10.1126/science.275.5296.54.

[42] J.-L. Heully, F. Alary, M. Boggio-Pasqua, Spin-orbit effects on the photophysical properties of $Ru(bpy)_3^{2+}$, J. Chem. Phys. 131 (2009) 184308. https://doi.org/10.1063/1.3254196.

[43] T. Petrenko, F. Neese, Analysis and prediction of absorption band shapes, fluorescence band shapes, resonance Raman intensities, and excitation profiles using the time-dependent theory of electronic spectroscopy, J. Chem. Phys. 127 (2007) 164319. https://doi.org/10.1063/1.2770706.

[44] T. Petrenko, F. Neese, Efficient and automatic calculation of optical band shapes and resonance Raman spectra for larger molecules within the independent mode displaced harmonic oscillator model, J. Chem. Phys. 137 (2012) 234107.

[45] A. Soupart, I.M. Dixon, F. Alary, J.-L. Heully, DFT rationalization of the room-temperature luminescence properties of $Ru(bpy)_3^{2+}$ and $Ru(tpy)_2^{2+}$: ^{3}MLCT–^{3}MC minimum energy path from NEB calculations and emission spectra from VRES calculations, Theor. Chem. Acc. 137 (2018). https://doi.org/10.1007/s00214-018-2216-1.

[46] L. Farouil, F. Alary, E. Bedel-Pereira, J.-L. Heully, Revisiting the Vibrational and Optical Properties of P3HT: A Combined Experimental and Theoretical Study, J. Phys. Chem. A. 122 (2018) 6532–6545. https://doi.org/10.1021/acs.jpca.8b03814.

[47] C. Kreitner, K. Heinze, Excited state decay of cyclometalated polypyridine ruthenium complexes: insight from theory and experiment, Dalton Trans. 45 (2016) 13631–13647. https://doi.org/10.1039/C6DT01989G.

[48] S. Essafi, J.N. Harvey, Rates of Molecular Vibrational Energy Transfer in Organic Solutions, J. Phys. Chem. A. 122 (2018) 3535–3540. https://doi.org/10.1021/acs.jpca.7b12563.

[49] F. Alary, J.-L. Heully, L. Bijeire, P. Vicendo, Is the ^{3}MLCT the Only Photoreactive State of Polypyridyl Complexes?, Inorg. Chem. 46 (2007) 3154–3165. https://doi.org/10.1021/ic062193i.

[50] S. Bonnet, J.-P. Collin, Ruthenium-based light-driven molecular machine prototypes: synthesis and properties, Chem. Soc. Rev. 37 (2008) 1207. https://doi.org/10.1039/b713678c.

[51] J.N. Harvey, M. Aschi, H. Schwarz, W. Koch, The Singlet and Triplet States of Phenyl Cation. A Hybrid Approach for Locating Minimum Energy Crossing Points Between Non-Interacting Potential Energy Syrfaces, Theor. Chem. Acc. 99 (1998) 95–99.

[52] J.N. Harvey, Spin-forbidden reactions: computational insight into mechanisms and kinetics: Spin-forbidden reactions, Wiley Interdiscip. Rev. Comput. Mol. Sci. 4 (2014) 1–14. https://doi.org/10.1002/wcms.1154.

[53] J.N. Harvey, Computational Studies of Reactivity in Transition Metal Chemistry, in: Phys. Inorg. Chem. Princ. Methods Models, Bakac, Andreja, 2010: pp. 459–499.

[54] J.P. Malhado, J.T. Hynes, Non-adiabatic transition probability dependence on conical intersection topography, J. Chem. Phys. 145 (2016) 194104. https://doi.org/10.1063/1.4967259.

[55] A.J. Göttle, I.M. Dixon, F. Alary, J.-L. Heully, M. Boggio-Pasqua, Adiabatic Versus Nonadiabatic Photoisomerization in Photochromic Ruthenium Sulfoxide Complexes: A Mechanistic Picture from Density Functional Theory Calculations., J. Am. Chem. Soc. 133 (2011) 9172–9174. https://doi.org/10.1021/ja201625b.

[56] E. Lebon, S. Bastin, P. Sutra, L. Vendier, R.E. Piau, I.M. Dixon, M. Boggio-Pasqua, F. Alary, J.-L. Heully, A. Igau, A. Juris, Can a functionalized phosphineligand promote room temperature luminescence of the $[Ru(bpy)(tpy)]^{2+}$ core?, Chem Commun. 48 (2012) 741–743. https://doi.org/10.1039/C1CC15737J.

[57] A. Breivogel, M. Meister, C. Förster, F. Laquai, K. Heinze, Excited State Tuning of Bis(tridentate) Ruthenium(II) Polypyridine Chromophores by Push-Pull Effects and Bite Angle Optimization: A Comprehensive Experimental and Theoretical Study, Chem. - Eur. J. 19 (2013) 13745–13760. https://doi.org/10.1002/chem.201302231.

[58] T. Österman, M. Abrahamsson, H.-C. Becker, L. Hammarström, P. Persson, Influence of Triplet State Multidimensionality on Excited State Lifetimes of Bis-tridentate Ru(II) Complexes: A Computational Study, J. Phys. Chem. A. 116 (2012) 1041–1050. https://doi.org/10.1021/jp207044a.

[59] Q. Sun, B. Dereka, E. Vauthey, L.M. Lawson Daku, A. Hauser, Ultrafast transient IR spectroscopy and DFT calculations of ruthenium(II) polypyridyl complexes, Chem. Sci. 8 (2017) 223–230. https://doi.org/10.1039/C6SC01220E.

[60] H. Jonsson, G. Mills, K.W. Jacobsen, Nudged Elastic Band Method for Finding Minimum Energy Paths of Transitions, in: Class. Quantum Dyn. Condens. Phase Simul., Berne B. J., Ciccoti G. and Coker D. F., 1998: pp. 385–404.

[61] G. Henkelman, G. Johannesson, H. Jonsson, Methods for Finding Saddle Points and Minimum Energy Paths, in: Prog. Theor. Chem. Phys., Schwartz S. D., 2000: pp. 269–302.

[62] S. Smidstrup, A. Pedersen, K. Stokbro, H. Jónsson, Improved initial guess for minimum energy path calculations, J. Chem. Phys. 140 (2014) 214106.

[63] F. Alary, M. Boggio-Pasqua, J.-L. Heully, C.J. Marsden, P. Vicendo, Theoretical Characterization of the Lowest Triplet Excited States of the Tris-(1,4,5,8-tetraazaphenanthrene) Ruthenium Dication Complex, Inorg. Chem. 47 (2008) 5259–5266. https://doi.org/10.1021/ic800246t.

[64] J.V. Caspar, T.J. Meyer, Photochemistry of $Ru(bpy)_3^{2+}$. Solvent Effects, J. Am. Chem. Soc. 105 (1983) 5583–5590.

[65] A. Amini, A. Harriman, A. Mayeux, The triplet excited state of ruthenium(II) bis(2,2′:6′,2″-terpyridine): Comparison between experiment and theory, Phys Chem Chem Phys. 6 (2004) 1157–1164. https://doi.org/10.1039/B313526H.

[66] A. Bahreman, B. Limburg, M.A. Siegler, E. Bouwman, S. Bonnet, Spontaneous Formation in the Dark, and Visible Light-Induced Cleavage, of a Ru–S Bond in Water: A Thermodynamic and Kinetic Study, Inorg. Chem. 52 (2013) 9456–9469. https://doi.org/10.1021/ic401105v.

[67] A.J. Göttle, F. Alary, M. Boggio-Pasqua, I.M. Dixon, J.-L. Heully, A. Bahreman, S.H.C. Askes, S. Bonnet, Pivotal Role of a Pentacoordinate ^{3}MC State on the Photocleavage Efficiency of a Thioether Ligand in Ruthenium(II) Complexes: A Theoretical Mechanistic Study, Inorg. Chem. 55 (2016) 4448–4456. https://doi.org/10.1021/acs.inorgchem.6b00268.

[68] B.S. Howerton, D.K. Heidary, E.C. Glazer, Strained Ruthenium Complexes Are Potent Light-Activated Anticancer Agents, J. Am. Chem. Soc. 134 (2012) 8324–8327. https://doi.org/10.1021/ja3009677.

[69] D.F. Azar, H. Audi, S. Farhat, M. El-Sibai, R.J. Abi-Habib, R.S. Khnayzer, Phototoxicity of strained Ru(II) complexes: is it the metal complex or the dissociating ligand?, Dalton Trans. 46 (2017) 11529–11532. https://doi.org/10.1039/C7DT02255G.

[70] J.-A. Cuello-Garibo, M.S. Meijer, S. Bonnet, To cage or to be caged? The cytotoxic species in ruthenium-based photoactivated chemotherapy is not always the metal, Chem. Commun. 53 (2017) 6768–6771. https://doi.org/10.1039/C7CC03469E.

[71] G. Li, M.D. Brady, G.J. Meyer, Visible Light Driven Bromide Oxidation and Ligand Substitution Photochemistry of a Ru Diimine Complex, J. Am. Chem. Soc. 140 (2018) 5447–5456. https://doi.org/10.1021/jacs.8b00944.

[72] J.-A. Cuello-Garibo, E. Pérez-Gallent, L. van der Boon, M.A. Siegler, S. Bonnet, Influence of the Steric Bulk and Solvent on the Photoreactivity of Ruthenium Polypyridyl

Complexes Coordinated to L-Proline, Inorg. Chem. 56 (2017) 4818–4828. https://doi.org/10.1021/acs.inorgchem.6b02794.

[73] E. Baranoff, J.-P. Collin, Y. Furusho, A.-C. Laemmel, J.-P. Sauvage, A photochromic system based on photochemical or thermal chelate exchange on Ru(phen)2L2+ (L = diimine or dinitrile ligand), Chem. Commun. (2000) 1935–1936. https://doi.org/10.1039/b004982o.

[74] A.-C. Laemmel, J.-P. Collin, J.-P. Sauvage, G. Accorsi, N. Armaroli, Macrocyclic Complexes of $[Ru(N\text{-}N)_2]^{2+}$ Units [N-N= 1, 10 Phenanthroline or 4-(p-Anisyl)-1, 10-Phenanthroline]: Synthesis and Photochemical Expulsion Studies, Eur. J. Inorg. Chem. 2003 (2003) 467–474.

[75] P. Mobian, J.-M. Kern, J.-P. Sauvage, Light-Driven Machine Prototypes Based on Dissociative Excited States: Photoinduced Decoordination and Thermal Recoordination of a Ring in a Ruthenium(II)-Containing[2]Catenane, Angew. Chem. Int. Ed. 43 (2004) 2392–2395. https://doi.org/10.1002/anie.200352522.

[76] J.-P. Collin, D. Jouvenot, M. Koizumi, J.-P. Sauvage, Light-Driven Expulsion of the Sterically Hindering Ligand L in Tris-diimine Ruthenium(II) Complexes of the $Ru(phen)_2(L)^{2+}$ Family: A Pronounced Ring Effect, Inorg. Chem. 44 (2005) 4693–4698. https://doi.org/10.1021/ic050246a.

[77] P.A. Scattergood, P.I.P. Elliott, An unexpected journey from highly tunable phosphorescence to novel photochemistry of 1,2,3-triazole-based complexes, Dalton Trans. 46 (2017) 16343–16356. https://doi.org/10.1039/C7DT03836D.

[78] P.A. Scattergood, A. Sinopoli, P.I.P. Elliott, Photophysics and photochemistry of 1,2,3-triazole-based complexes, Coord. Chem. Rev. 350 (2017) 136–154. https://doi.org/10.1016/j.ccr.2017.06.017.

[79] C.E. Welby, S. Grkinic, A. Zahid, B.S. Uppal, E.A. Gibson, C.R. Rice, P.I.P. Elliott, Synthesis, characterisation and theoretical study of ruthenium 4,4′-bi-1,2,3-triazolyl complexes: fundamental switching of the nature of S_1 and T_1 states from MLCT to MC, Dalton Trans. 41 (2012) 7637. https://doi.org/10.1039/c2dt30510k.

[80] C.E. Welby, C.R. Rice, P.I.P. Elliott, Unambiguous Characterization of a Photoreactive Ligand-Loss Intermediate, Angew. Chem. Int. Ed. 52 (2013) 10826–10829. https://doi.org/10.1002/anie.201304219.

[81] C.E. Welby, G.K. Armitage, H. Bartley, A. Sinopoli, B.S. Uppal, P.I.P. Elliott, Photochemical ligand ejection from non-sterically promoted Ru(II)bis(diimine) 4,4′-bi-1,2,3-triazolyl complexes, Photochem Photobiol Sci. 13 (2014) 735–738. https://doi.org/10.1039/C3PP50437A.

[82] J. Van Houten, R.J. Watts, Photochemistry of Tris(2,2'-bipyridyl)ruthenium(II) in Aqueous Solution, Inorg. Chem. 17 (1978) 3381–3385.

[83] S. Tachiyashiki, K. Nakamaru, K. Mizumachi, A Long-Lived Intermediate with a Unidentate Dmbpy Ligand in the Photosubstitution of $[Ru(bpy)_2(dmbpy)]^{2+}$ (dmbpy=3,3'-dimethyl-2,2'-bipyridine), Chem. Lett. (1992) 1119–1122.

[84] S. Tachiyashiki, H. Ikezawa, K. Mizumachi, Identification of an Intermediate of the Photosubstitution of a Ruthenium(II) Diimine Complex With a Monodentate Chelating Ligand: ^1H NMR and HPLC Evidence, Inorg. Chem. 33 (1994) 623–625.

[85] D.W. Thompson, J.F. Wishart, B.S. Brunschwig, N. Sutin, Efficient Generation of the Ligand Field Excited State of Tris-(2,2‘-bipyridine)-ruthenium(II) through Sequential Two-Photon Capture by $[Ru(bpy)_3]^{2+}$ or Electron Capture by $[Ru(bpy)_3]^{3+}$, J. Phys. Chem. A. 105 (2001) 8117–8122. https://doi.org/10.1021/jp011854o.

[86] C.E. Welby, G.K. Armitage, H. Bartley, A. Wilkinson, A. Sinopoli, B.S. Uppal, C.R. Rice, P.I.P. Elliott, Photochemistry of Ru(II) 4,4′-Bi-1,2,3-triazolyl (btz) Complexes: Crystallographic Characterization of the Photoreactive Ligand-Loss Intermediate *trans*-$[Ru(bpy)(\kappa^2\text{-btz})(\kappa^1\text{-btz})(NCMe)]^{2+}$, Chem. - Eur. J. 20 (2014) 8467–8476. https://doi.org/10.1002/chem.201402354.

[87] I.M. Dixon, J.-L. Heully, F. Alary, P.I.P. Elliott, Theoretical illumination of highly original photoreactive ^{3}MC states and the mechanism of the photochemistry of Ru(II) tris(bidentate) complexes, Phys Chem Chem Phys. 19 (2017) 27765–27778. https://doi.org/10.1039/C7CP05532C.

[88] L.G. Vanquickenborne, A. Ceulemans, Ligand-Field Models and the Photochemistry of Coordination Compounds, Coord. Chem. Rev. 48 (1983) 157–202.

[89] Ph. Wernet, K. Kunnus, I. Josefsson, I. Rajkovic, W. Quevedo, M. Beye, S. Schreck, S. Grübel, M. Scholz, D. Nordlund, W. Zhang, R.W. Hartsock, W.F. Schlotter, J.J. Turner, B. Kennedy, F. Hennies, F.M.F. de Groot, K.J. Gaffney, S. Techert, M. Odelius, A. Föhlisch, Orbital-specific mapping of the ligand exchange dynamics of $Fe(CO)_5$ in solution, Nature. 520 (2015) 78–81. https://doi.org/10.1038/nature14296.

[90] M. Reinhard, G. Auböck, N.A. Besley, I.P. Clark, G.M. Greetham, M.W.D. Hanson-Heine, R. Horvath, T.S. Murphy, T.J. Penfold, M. Towrie, M.W. George, M. Chergui, Photoaquation Mechanism of Hexacyanoferrate(II) Ions: Ultrafast 2D UV and Transient Visible and IR Spectroscopies, J. Am. Chem. Soc. 139 (2017) 7335–7347. https://doi.org/10.1021/jacs.7b02769.

[91] J.M. Żurek, M.J. Paterson, Photostereochemistry and Photoaquation Reactions of $[Cr(tn)_3]^{3+}$: Theoretical Studies Show the Importance of Reduced Coordination Conical Intersection Geometries, J. Phys. Chem. A. 116 (2012) 5375–5382. https://doi.org/10.1021/jp302300q.

[92] A. Juris, V. Balzani, F. Barigelletti, S. Campagna, P. l Belser, A. Von Zelewsky, Ru(II) polypyridine complexes: photophysics, photochemistry, eletrochemistry, and chemiluminescence, Coord. Chem. Rev. 84 (1988) 85–277.

[93] P.E. Hoggard, G.B. Porter, Photoanation of the Tris(2,2’-bipyridine)ruthenium(II) Cation by Thiocyanate, J. Am. Chem. Soc. 100 (1978) 1457–1463.

[94] Q. Sun, S. Mosquera-Vazquez, L.M. Lawson Daku, L. Guénée, H.A. Goodwin, E. Vauthey, A. Hauser, Experimental Evidence of Ultrafast Quenching of the ^{3}MLCT Luminescence in Ruthenium(II) Tris-bipyridyl Complexes via a ^{3}dd State, J. Am. Chem. Soc. 135 (2013) 13660–13663. https://doi.org/10.1021/ja407225t.

[95] K. Onda, T. Mukuta, S. Tanaka, K. Murata, A. Inagaki, Observation of the dark state in ruthenium complexes using femtosecond infrared vibrational spectroscopy, in: Int. Conf. Ultrafast Phenom., Optical Society of America, 2014: p. 11.Fri.A.7.

[96] T. Mukuta, S. Tanaka, A. Inagaki, S. Koshihara, K. Onda, Direct Observation of the

Triplet Metal-Centered State in $[Ru(bpy)_3]^{2+}$ Using Time-Resolved Infrared Spectroscopy, ChemistrySelect. 1 (2016) 2802–2807. https://doi.org/10.1002/slct.201600747.

[97] A. Soupart, F. Alary, J.-L. Heully, P.I.P. Elliott, I.M. Dixon, Exploration of Uncharted ^{3}PES Territory for $[Ru(bpy)_3]^{2+}$: A New ^{3}MC Minimum Prone to Ligand Loss Photochemistry, Inorg. Chem. 57 (2018) 3192–3196. https://doi.org/10.1021/acs.inorgchem.7b03229.

[98] L. Feng, Y. Wang, J. Jia, Triplet Ground-State-Bridged Photochemical Process: Understanding the Photoinduced Chiral Inversion at the Metal Center of $[Ru(phen)_2(L\text{-ser})]^+$ and Its Bipy Analogues, Inorg. Chem. 56 (2017) 14467–14476. https://doi.org/10.1021/acs.inorgchem.7b02030.

[99] D. Jacquemin, D. Escudero, The short device lifetimes of blue PhOLEDs: insights into the photostability of blue Ir(III) complexes, Chem Sci. 8 (2017) 7844–7850. https://doi.org/10.1039/C7SC03905K.

[100] S. Arroliga-Rocha, D. Escudero, Facial and Meridional Isomers of Tris(bidentate) Ir(III) Complexes: Unravelling Their Different Excited State Reactivity, Inorg. Chem. 57 (2018) 12106–12112. https://doi.org/10.1021/acs.inorgchem.8b01675.

[101] D. Escudero, *Mer*-$Ir(ppy)_3$ to *Fac*-$Ir(ppy)_3$ Photoisomerization, ChemPhotoChem. 3 (2019) 697–701. https://doi.org/10.1002/cptc.201900029.

[102] Y. Rojas Pérez, L.D. Slep, R. Etchenique, *Cis–Trans* Interconversion in Ruthenium(II) Bipyridine Complexes, Inorg. Chem. 58 (2019) 11606–11613. https://doi.org/10.1021/acs.inorgchem.9b01485.

[103] P.A. Scattergood, D.A.W. Ross, C.R. Rice, P.I.P. Elliott, Labilizing the Photoinert: Extraordinarily Facile Photochemical Ligand Ejection in an $[Os(N\hat{}N)_3]^{2+}$ Complex, Angew. Chem. Int. Ed. 55 (2016) 10697–10701. https://doi.org/10.1002/anie.201604959.

[104] L.X. Chen, X. Zhang, M.L. Shelby, Recent advances on ultrafast X-ray spectroscopy in the chemical sciences, Chem Sci. 5 (2014) 4136–4152. https://doi.org/10.1039/C4SC01333F.

[105] M. Chergui, E. Collet, Photoinduced Structural Dynamics of Molecular Systems Mapped by Time-Resolved X-ray Methods, Chem. Rev. 117 (2017) 11025–11065. https://doi.org/10.1021/acs.chemrev.6b00831.

[106] K.S. Kjær, T.B. Van Driel, T.C.B. Harlang, K. Kunnus, E. Biasin, K. Ledbetter, R.W. Hartsock, M.E. Reinhard, S. Koroidov, L. Li, M.G. Laursen, F.B. Hansen, P. Vester, M. Christensen, K. Haldrup, M.M. Nielsen, A.O. Dohn, M.I. Pápai, K.B. Møller, P. Chabera, Y. Liu, H. Tatsuno, C. Timm, M. Jarenmark, J. Uhlig, V. Sundström, K. Wärnmark, P. Persson, Z. Németh, D.S. Szemes, É. Bajnóczi, G. Vankó, R. Alonso-Mori, J.M. Glownia, S. Nelson, M. Sikorski, D. Sokaras, S.E. Canton, H.T. Lemke, K.J. Gaffney, Finding intersections between electronic excited state potential energy surfaces with simultaneous ultrafast X-ray scattering and spectroscopy, Chem. Sci. 10 (2019) 5749–5760. https://doi.org/10.1039/C8SC04023K.